

STUDY ON RESIDUAL STRESS AND STRAIN DURING RAIL ROLLING CONTACT OF STRAIGHT U75V RAIL

Received – Primljeno: 2018-10-31

Accepted – Prihvaćeno: 2019-02-15

Original Scientific Paper – Izvorni znanstveni rad

The distribution of residual stress produced by straightening process in side the rail is obtained. And then the residual stress result is used as the initial condition to study the stress and strain variation rule of wheel-rail rolling contact process. Results shows that with the increase of rolling times, the straightening residual stress of rail quickly redistributed and gradually stabilized. The residual stress of rail head is mainly affected by wheel rolling, while the rail waist and bottom is mainly affected by straightening. The effect of straightening residual stress on residual shear stain is relatively small.

Key words: U75 Rail, wheel rolling, straight rail, stress, strain

INTRODUCTION

The distribution of rail residual stress and strain directly affects the service life of rail and the driving safety of the train[1]. Residual stress produced by hot rolling-cooling and straightening processes has an important influence on the wear resistance, fatigue strength and fracture resistance of the rail in service, it is one of the key factors determining the average cyclic fatigue stress of the rail[2]. The residual stress produced by production process and wheel rolling process together determine the stress and strain distribution of rail. Therefore, it is necessary to study the variation of the stress and strain of rail during wheel rolling on the premise of considering the residual stress of production.

Scholars have done a lot of research on the contact process between wheel and rail, but seldom considered the influence of the production residual stress. In this paper, an elastic finite element method for calculating the residual stresses in rail production is presented, and the wheel rolling stresses and strains of straight rail are studied on the basis of considering the production residual stresses and cyclic plastic constitutive models.

CALCULATION OF RESIDUAL STRESS IN PRODUCTION

The residual stress produced by hot rolling and cooling process has little affect on straightening residual stress[3], this paper only considered the straightening

process when studying the residual stress in production. The rail straightening machine consists of 9 horizontal rollers and 8 vertical rollers, the rolling reduction of straightening rollers is shown in Table 1. In simulation model, the straightening roller is described as rigid-body and the rail is set at Bilinear-Hardened-Material model. The version of rail is U75V 60 kg/m, its parameters are determined by experiment, the modulus of elasticity is 2,05e5 MPa, the shear elasticity is 1,18e4 MPa, the yield strength is 525 MPa, and the Poisson's ratio is 0,3. C3D8R (8-node, linear, hexahedron, reduction integral, 3D stress) element and R3D4D (4-node, bilinear, quadrilateral, 3D rigid body) element are used to mesh the rail and straightening roller respectively. The friction coefficient between the rail and the roller is set to 0,3, and the Global -Contact is used to establish the interaction relationship. The rotating speeds of the horizontal and vertical rolls are 3 rad/s and 4,5 rad/s, respectively. The rail is set at 1 800 initial speed to enter the straightening roller, and then the rail is moved by the friction force of the roller. The object time increment for mass scaling is set to 5,98e-5 s.

Table 1 **Rolling reduction of straightening rollers**

name	Horizontal roller				Vertical roller		
number Roller	2#	4#	6#	8#	11#	13#	15#
Intermesh/mm	19,2	11,2	7,9	3,5	12	6	2,5

The middle position of the rail longitudinal direction is selected to define the node path (see Figure 1), and the straightening residual stress (if without special description, the residual stresses in this paper refer to the longitudinal residual stresses) of this path as shown in Figure 2 It can be seen from the Figure 2 that the distribution of residual stress produced by rail straightening

M. X. Gao University of Science and Technology Liaoning, Innovative Pioneering and Engineering Training Center, Anshan city, China
H. Song, J. Yang, L. J. Fu: University of Science and Technology Liaoning, School of Mechanical Engineering and Automation, Anshan city, China
Corr. Author: e-mail:songhua88@126.com



Figure 1 The defined note path of the rail

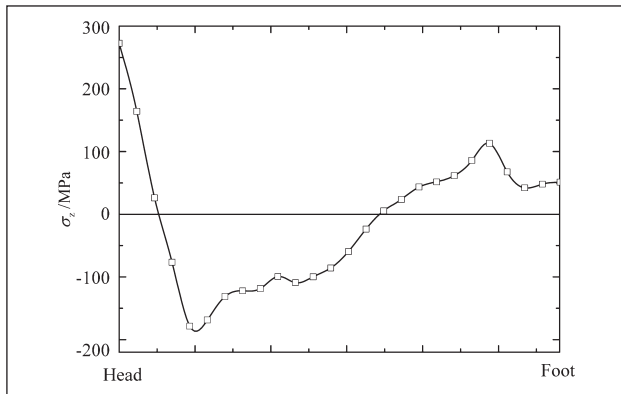


Figure 2 The straightening residual stress of rail on the path

looks like the shape of “C”, This result is basically the same as Chen Lin’s research[4].

FINITE ELEMENT MODEL OF WHEEL-RAIL ROLLING CONTACT

The Finite element model of wheel-rail rolling contact based on ABAQUS is shown in Figure 3. Only half of the models were built because of the symmetry of the straight track. The vertical stiffness damping and the firsts and seconds suspension system which are closely related to wheel-rail rolling contact frequency are introduced in the model. A discrete single-layer supporting track dynamic model are used under the rail. The vertical stiffness of the fastener is the sum of the vertical stiffness of the rectangular rubber cushion and the vertical stiffness of the fastener. The Stiffness of track bed is calculated by single layer ballast stiffness calculation method. The constitutive model of nonlinear follow-up hardening material is used for both wheel and rail in order to consider the ratcheting effect of rail under cyclic wheel loads. The constitutive model also considers the cyclic hardening and mean stress relaxation caused by Singer effect and plastic shakedown. The relationship between semi periodic plastic strain and true stress

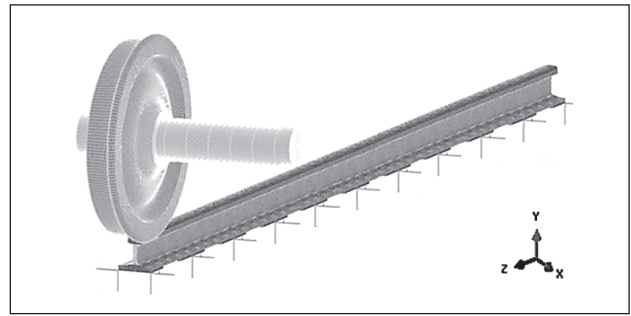


Figure 3 The finite element model of wheel-rail rolling contact

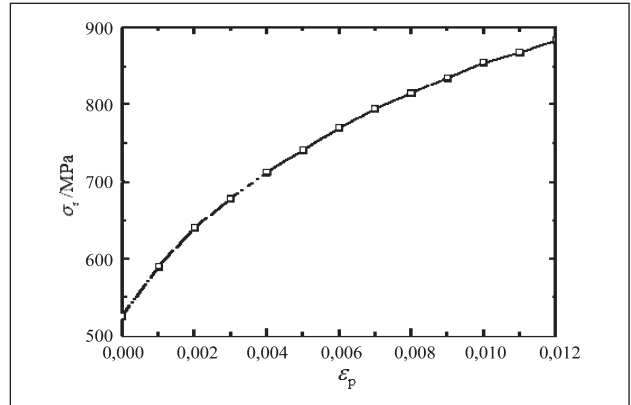


Figure 4 The plastic strain-real stress curve of rail

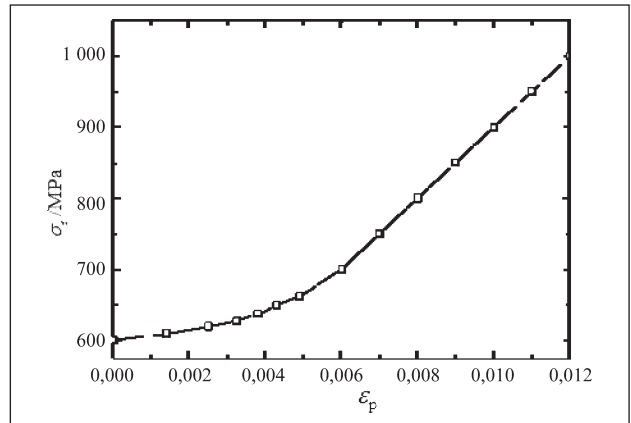


Figure 5 The plastic strain-real stress curve of wheel

of wheel and rail materials is shown in Figures 4 and 5 respectively. The C3D8R element is used to mesh the rail and wheel. The algorithm of surface-surface function contact constraint is used to describe the wheel-rail rolling contact behavior.

The elastic modulus of wheel / rail materials is set to 2,05e5 MPa and the poisson’s ratio is set to 0,28. For simulation parameters: the wheel rolling speed is set to $v = 200$ km/h, the axle load is set to 14t, the longitudinal creep rate is set to 0,001, and the friction coefficient between wheel and rail is set to 0,3.

RESULTS AND DISCUSSION

For convenience of distinguishing and displaying, “RS rail” is used to express the rail with straightening

residual stress and “SF rail” is used to express the rails of stress free, and “H” is defined as the distance from the point on the track (as shown in Figure 2) to the top of the rail tread.

Results of RS rail

Figures 6 and 7 show the variation of residual stress σ_z of the RS rail on the path and at different H values during 20 cycles of wheel rolling, respectively.

The curve 0 in Figure 6 indicates the straightening residual stress of rail. The Figure 6 shows that the rolling of the wheel will quickly change the residual stress distribution of RS rails and redistribute them, and there can be seen obvious tension and compression changes in the range of $H = 0 - 8$ mm. After 20 cycles of wheel rolling, the residual stress of rail is compressive stress in the range of $H = 0 - 8$ mm, tensile stress in the range of $H = 8 - 18$ mm, compressive stress in the range of $H = 18 - 100$ mm and tensile stress in the range of $H > 100$ mm. After each wheel rolling, the maximum residual compressive stress of rail appears at $H \approx 3,52$ mm and the maximum residual tensile stress of rail appears at Rail bottom ($H = 176$ mm). Figure 7 shows that with the increase of wheel rolling times, the residual stress decreases gradually at $H = 0$ mm and $H = 3,52$ mm, and increases gradually at $H = 12,32$ mm, and the variation rate is decreasing. It can be concluded that after 20 cy-

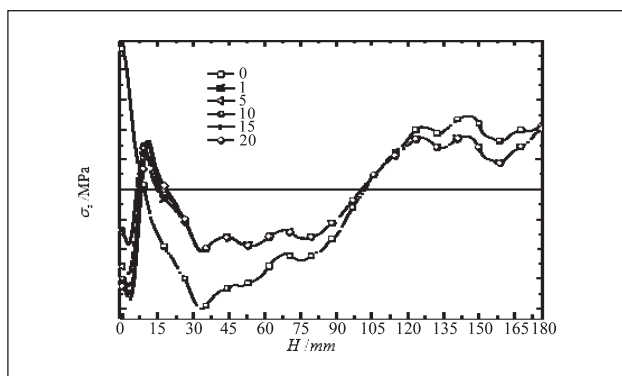


Figure 6 Variation of residual stress σ_z of RS rail rolling contact process rolling contact process

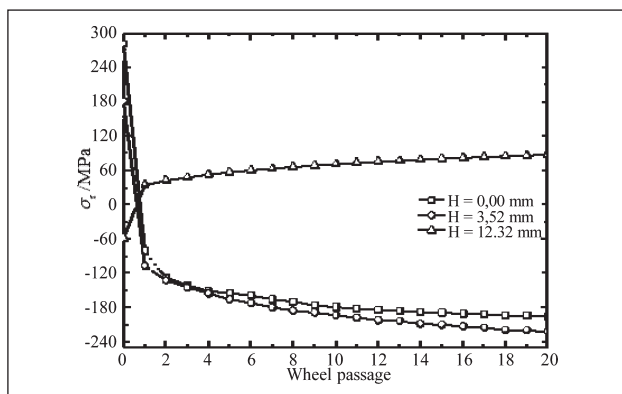


Figure 7 Variation of residual stress σ_z of RS rail at different H values

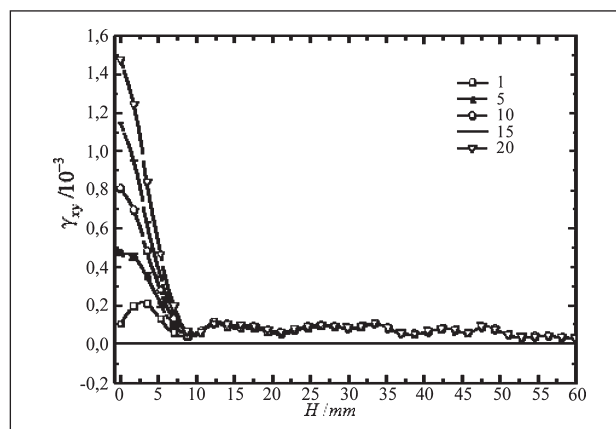


Figure 8 Variation of residual shear strain γ_{xy} of RS rail

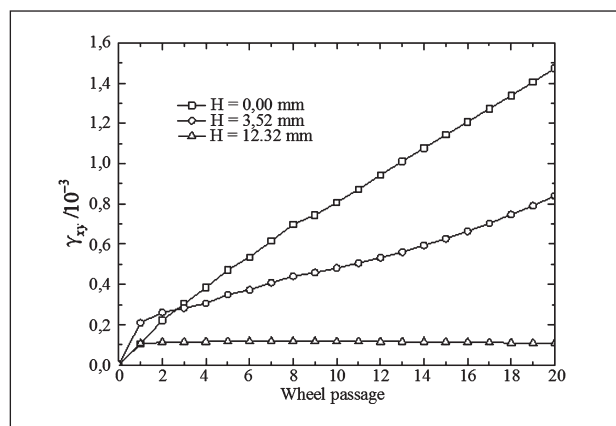


Figure 9 Variation of residual shear strain γ_{xy} at different H values of RS rail

cles of rolling, the amplitude and rate of residual stress variation at all parts of the rail are in a small level. It is basically in a stable state.

Figures 8 and 9 show the variation of residual shear strain γ_{xy} of the RS rail on the path and at different H values during 20 cycles of wheel rolling, respectively.

Figure 8 shows that the rail presents tensile strain in the range of $H = 0 - 62$ mm and shows compressive strain at $H > 62$ mm. During 20 cycles of rolling, the residual shear strain γ_{xy} of the rail changes obviously only in the range of $H = 0 - 10$ mm. In addition, with the increase of rolling times, the location of the maximum residual shear strain of the rail changes gradually from $H = 3,52$ mm to $H = 0$ mm. Figure 9 shows that the residual shear strain at $H = 0$ mm and $H = 3,52$ mm increases linearly with the increase of rolling times, and the residual shear strain keeps increasing and does not tend to be stable after 20 cycles of rolling.

Comparative between RS rail and SF rail

Figures 10 and 11 show the results of residual stress σ_z and residual shear strain γ_{xy} on the path of RS rail and SF rail after 20 cycles of rolling contact, respectively.

It can be seen from Figures that the change regulation of residual stresses of RS rail and SF rail are basically the same in the range of $H = 0 - 18$ mm after 20

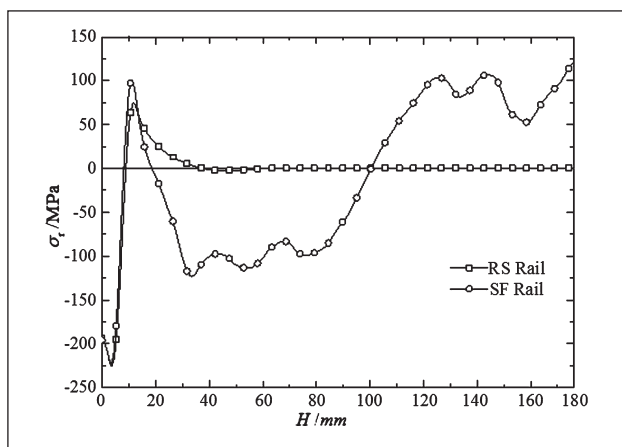


Figure 10 Comparison of residual stress σ_z of SF and RS rail after 20 cycles of rolling contact

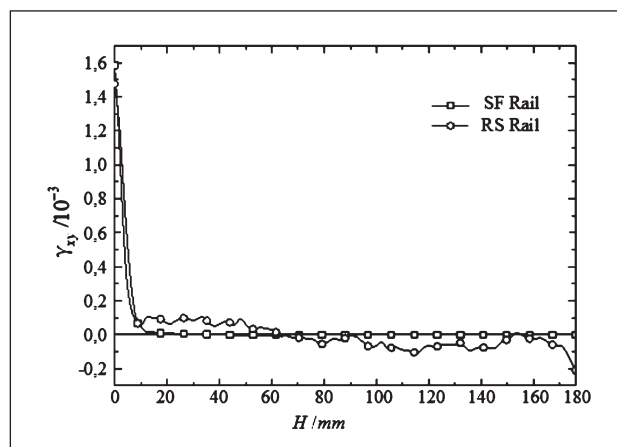


Figure 11 Comparison of residual shear strain γ_{xy} of SF and RS rail after 20 cycles of rolling contact

rolling cycles, except in the numerical value. The difference of residual stresses for the two kind of rails at $H = 0$ mm, $H = 3,52$ mm, $H = 12,32$ mm is -2,13 MPa, 2,84 MPa and 13,77 MPa, respectively. It can be concluded that the effect of straightening residual stress on residual shear strain of rail is relatively small.

CONCLUSION

With the increase of wheel rolling times, the production residual stress σ_z of straight rail is redistributed quickly and tends to be stable gradually. The rolling effect of the wheel at the rail head is greater than that of the production residual stress, while the production residual stress at the rail waist and rail bottom is greater than that of the wheel rolling effect.

With the increase of rolling times, the residual shear strain γ_{xy} of the straight rail changes obviously only in the range of $H = 0 - 10$ mm, and has a gradually increasing trend. The residual shear strain at the rest positions of rail ($H > 10$ mm) are almost unchanged, and the

maximum position is shifted from $H = 3,52$ mm to $H = 0$ mm. The effect of straightening residual stress on the residual shear strain of the rail during service is relatively small.

REFERENCES

- [1] S. H. Cao, X-Li, S. F. Zhang, Research of the Differences between Hertz Theory and Finite Element Method to Analyze the Fatigue of Wheel/Rail Contact, *Journal of Mechanical Engineering* 51(2015)06,126-134.
- [2] G. Schleinzer, F. D. Fischer. Residual stress formation during the roller straightening of railway rails. *International Journal of Mechanical Sciences* 43(2001)10, 2281-2295.
- [3] J. W. Ringsberg, T. Lindbäck. Rolling contact fatigue analysis of rails including numerical simulations of the rail manufacturing process and repeated wheel-rail contact loads. *International Journal of fatigue* 25(2003)6, 547-558.
- [4] L. Chen, B. Y. Wang, Z. Z. Wu, An Investigation for Residual Stress of High-Speed Rails Due to Roller Straightening, *Iron and Steel* 41(2006)2, 451-456

Note: J. Yang is responsible for English language, Anshan, China